



A simple thermodynamic approach to predict responses from polymer-coated quartz crystal microbalance sensors exposed to organic vapors

P. Palmas^{a,*}, J. Klingenfus^a, B. Vedeau^a, E. Girard^a, P. Montmeat^a, L. Hairault^a, C.M. Pradier^b, C. Méthivier^b

^a CEA, DAM, Le Ripault, F-37260 Monts, France

^b UPMC, Université Paris VI, Laboratoire de Réactivité de Surfaces, UMR CNRS 7197, F-75005 Paris, France

ARTICLE INFO

Article history:

Received 12 April 2013

Received in revised form

5 June 2013

Accepted 12 June 2013

Available online 18 June 2013

Keywords:

Chemical sensor

QCM

Polysiloxane

NMR

PM-IRRAS

Sorption enthalpy

Intermolecular interaction

ABSTRACT

As of lately, the demand for developing artificial sensors with improved capabilities for the detection of explosives, toxics or drugs has increased. Ideally, sensor devices should provide high sensitivity and give a response that is specific to a given target molecule without being influenced by possible interfering molecules in the atmosphere. These properties strongly depend on the structure of the chemical compound used as a sensitive material. It is thus crucial to select the right compound and this step would be facilitated with the aid of predictive tools. The present investigations have been focused on a family of functionalized polysiloxane polymers deposited on a QCM device, producing only weak interactions compatible with reversible sensors. The quartz frequency variation at equilibrium has been linked to the partition coefficient that was evaluated using a thermodynamic description of the adsorption process. We have shown that the relative responses of two polymers can be directly determined from the Gibbs free enthalpy of mixing as determined from NMR measurements performed on neat liquid mixtures. An equivalence of this term—including both enthalpy and entropy contributions—to the energy interaction term calculated using Hansen solubility coefficients, has been demonstrated previously. These results constitute a basis for the development of a numerical program for calculating equilibrium sensor responses. For small molecules, the adsorption kinetics can be easily accounted for by a Fick diffusion coefficient estimated from the Van der Waals volume.

© 2013 Elsevier B.V. All rights reserved.

1. Introduction

Examples of application fields for gas chemical sensors include preventing terrorism against populations, averting the exposure to pollutants in the workplace, at home or in the city, and impeding the traffic in illicit products [1]. A very sophisticated version of such a device has been elaborated by nature itself: the olfactory system. Hence, the use of dogs remains the most efficient technique for detecting explosives, toxics or drugs [2]. However, the method is not universal and its extension to a large panel of applications is not possible because of the time required for the training of dogs and the reduced period of practical use.

As a consequence, proposing new strategies for the development of artificial sensors with improved capabilities has become of prime importance. Ideal sensors are very sensitive and specific to a given target molecule (hereafter denoted as analyte), and at the same time

insensitive to the various gases (interfering molecules) released in the atmosphere by natural or manufactured products like fragrances, cosmetics, plastics. In practice, a layer of sensitive material supported by a receptor device is exposed to a gas phase. Hence, once the analyte is adsorbed, some property of the layer is modified and consecutively transformed into a detectable signal by a transduction system.

The development of a sensor with specific properties for a given application depends on many experimental parameters including the transduction system, the deposited layer characteristics, the geometry, the signal level and shape. The chemical structure of the sensitive material is certainly the parameter offering the broadest panel of possibilities [3]. The selection of the compound with the desired property can be made empirically or by means of a screening procedure. However, due to cost and time limitations, a more rational strategy is required.

Research undertaken in our laboratory has been devoted to the development of reversible sensors compatible with several utilizations. The present investigations were thus restricted to sensitive materials producing weak interactions that exclude covalent binding. In this field, the high potential of functionalized

* Corresponding author. Tel.: +33 247344000; fax: +33 247345148.
E-mail address: pascal.palmas@cea.fr (P. Palmas).

polysiloxane systems, of which the selectivity can be modulated by side chain selection, has already been demonstrated [4]. We also centered our research around this family of polymers which renders it possible to compare compounds with a variety of chemical functions, but with the same physical state and close rheological properties.

Since they are all viscous oils, the adsorption of the analyte is not restricted to the external surface of the sensitive material but potentially proceeds throughout its entire volume by diffusion. Consequently, physical properties like the porosity or the specific surface have only a second-order effect provided that the deposited layers of polymers are of similar nature. Moreover, many such chemical compounds are commercially available.

In the work of Hierlemann et al. [4], extensive temperature-dependent QCM measurements [5–7] of the partition coefficient were performed on a battery of compounds with seven polymers using a fully automated system. This led to the main conclusion that the adsorption is entropy-driven but the selectivity pattern is governed by the mixing enthalpy term. Our study employed a different QCM system and led to the proposal of a formalism enabling a thermodynamic evaluation of the sensor responses directly from the Gibbs free enthalpy of mixing including both enthalpy and entropy contributions. The main interest lies in the possibility of calculating this term from Hansen solubility coefficients that are highly documented. This strategy was built on the basis of NMR measurements performed independently on neat liquid mixtures [8] and in-situ PM-IRRAS [9] characterization of the adsorption on the deposited layer.

The present article thus proposes a comprehensive approach of several steps, theories and parameters governing the detection process. The main objective of the project was the development of numerical tools for predicting the sensor response as a function of the nature of the sensitive material and target molecules.

2. Material and methods

2.1. QCM measurements

For QCM measurements, Piezoelectric 9 MHz AT-cut quartz crystals were used (polished surface) with gold-plated metal electrodes on both sides. (AMETEK, model QA-A9M-AU M). A more detailed description of the whole apparatus is given in reference [10]. The two active surfaces of 0.39 cm² were coated with the sensitive materials. In these conditions, a frequency variation of 2 kHz corresponds to a mass variation of 4.2 µg in the Sauerbrey regime. Sensitive materials were spray-deposited on the gold surface using polymer solutions in chloroform (1.25 g/L). The applied pressure, the pipe aperture and the distance from the surface were optimized so as to obtain the desired coating after the rapid evaporation of the solvent. The deposited mass was measured from the quartz frequency variation, roughly proportional to the time of exposure to the spraying. The morphology of the coating was characterized by optical microscopy. The five polymers that have been evaluated, i.e. polycyanopropylmethylsiloxane, polyphenylmethylsiloxane, polyoctylmethylsiloxane, copoly-([(dimethylaminopropyl) carboxamidopyrrolidonyl] propylmethylsiloxane)-(dimethylsiloxane) and copoly-(pyrrolidonecarboxamidopropylmethylsiloxane)-(dimethylsiloxane) hereafter referred to as PCN, Pph, P8, PpyN and PpyCOO respectively, were from commercial provenance and used without any further purification.

In most cases, the spraying produced a distribution of small drops with different dimensions (in the range 1–10 µm) and shapes. A thinner and apparently continuous coating could only be obtained for ppyCOO and pyN, with some heterogeneities at the location of particles impurities. The thickness in that case was

estimated to less than 1 µm. The deposited layers were homogeneous except at the edges. Nevertheless, the contribution of this area is negligibly small as the sensitivity decreases exponentially as a function of the distance from the center of the quartz surface [5]. It is worth noticing that the deposition of a continuous and regular coating is not a prerequisite to perform a QCM measurement, unlike for other methods like SAW (surface acoustic wave detector) or resistivity measurements.

2.1.1. Experimental device

Since the pioneering work of King [6], several groups have investigated the sorption of gas in a material deposited on a QCM receptor. While most studies that reported on detection measurements have been performed in the presence of a gas flow, several groups still proceed with a static gas configuration. Generally, a gas mixture containing a calibrated concentration of analyte is prepared and introduced into an airtight glass compartment for detection [7].

A static protocol was employed also in the present investigation, but only compounds in their condensed phases were directly introduced, avoiding the tedious preparation of calibrated gas samples. A glass flask of 50 cm³ with two entries was utilized: (i) one for the QCM connected through a seal to ensure the airtightness of the system, and (ii) the second for the introduction of a calibrated amount of liquid/solid analyte to produce in situ the desired vapor concentration (after a short period of stabilization at ± 1 Hz).

Each experiment was followed by a desorption procedure in the air and the microbalances were kept in small airtight boxes free from pollutants. The flask was also systematically washed with acetone before being dried with dry neat nitrogen. The pollution level was controlled by measuring the QCM frequency. The sensitivity level was evaluated to a mass variation of 0.1% ($\Delta f = 2$ Hz that corresponds to 4.2 ng) for a polymer coating of 2 kHz. Each individual experiment was systematically repeated three times.

2.1.2. Introduction of the analyte

Liquid samples (a few µl) with a high P_{sat} were introduced directly through a septum with an electronic micro-syringe. The vapor concentration was then calculated assuming a complete vaporization inside the detection chamber. This holds as long as the resulting vapor pressure P_{vap} is lower than P_{sat} . The approach was thus not appropriate for nonvolatile compounds for which P_{sat} was reached with a liquid volume lower than the smallest that could be introduced, i.e., 0.2 µL which corresponds to 10,000 ppm. Hence, analytes presenting a P_{sat} lower than this limit were voluntarily introduced in excess (2 ml for liquids and 2 g for solids) by removing the septum. The time required to reach equilibrium was consequently reduced and the vapor pressure P_{vap} was assumed to be equal to P_{sat} .

2.2. PM-RAIRS measurements

PM-RAIRS measurements were carried out on an FT-IR spectrometer (Nicolet) coupled to a grid polarizer and a photoelastic modulator placed ahead of the sample to modulate the incident beam between *p* and *s* polarizations. The reflected light was focused on a nitrogen-cooled MCT wideband detector. The sum and difference interferograms were Fourier-transformed to yield the differential reflectivity $(R_p - R_s)/(R_p + R_s)$ which represents the PM-RAIRS spectrum. A Bessel function was used to remove the residual baseline deformation resulting from the phase modulation.

This technique provides the IR spectrum of a thin layer with an almost complete removal of any contribution from the gas phase.

We started using an IR beam with an incident angle of 85° which is optimum for a thin layer, and finally an optimization was performed manually by slightly rotating the sample and directly optimizing the signal intensity and the shape of the spectrum [9]. A series of spectra were acquired at 4 min intervals. The proportion of analyte adsorbed into the polymer was determined by spectral integration of one adsorption band of each species.

The samples were gold-plated blocks (1 cm by 1 cm) spray-coated according to the same protocol as described before, but with the amount of deposited polymer limited to a few hundred hertz. The blocks placed in the detection chamber were exposed to a nitrogen flow (26.5 L/h) containing a certain amount of analyte produced by bubbling or (in the case of solids) simply by contact. The actual concentration in the gas flow was determined by UV spectroscopy performed on an acetonitrile solution also produced by bubbling. A control was also possible following one of the individual IR spectra.

3. Results

3.1. QCM measurements

QCM (quartz crystal microbalance) is a quite simple system that is well known and has been widely used for detection purposes as well as other applications. The sensitive material deposited upon the crystal surface acts as a constraint modifying the quartz frequency. In practice, the mechanical oscillation is transmitted throughout the material and gradually damped upon a certain distance limit called the “skin thickness” d_s . This parameter is related to the density, ρ , the viscosity, η , and the frequency, ν , through the expression $d_s = (\eta/\pi\nu\rho)^{1/2}$.

In the case of an ideal rigid thin layer ($d < d_s$) that is well coupled to the surface, the movement of the crystal is entirely transmitted to the material. Detection tests being realized in the presence of vapor compounds, one may assume very weak dissipation of the adsorption energy, which is related to viscoelastic properties of the fluid. Sauerbrey [11] showed that the quartz frequency in this regime has a linear dependence on the mass of coated material. The case of a thick Newtonian fluid ($d > d_s$) is another interesting limit situation where the frequency is correlated to $\eta^{1/2}$. As the glass transition temperature T_g of coated polysiloxane oils is very low, these substances should in principle be considered as Maxwellian fluids, which corresponds to an intermediate situation. But it is well known that the effective T_g value depends on the frequency of the constraint that is applied to a polymer subjected to a periodic mechanical stress. A typical example is PDMS, for which the T_g shifts from -180°C (quasi static case) to 20°C at 10 MHz [12]. Therefore, for a correct interpretation of observed frequency variations one needs to address the issue of the relevant regime to be considered for QCM responses. Moreover, particular attention must be paid to possible modifications of the regime that may occur during detection following the adsorption of a large amount of gas.

3.1.1. Detection process

With a QCM sensor, the presence of a certain analyte (ideally the target molecule) is revealed by a variation of the quartz crystal frequency due to the transfer of this compound from the gas phase to the sensitive material. Both the frequency variation at equilibrium, Δf , and the kinetics depend on several parameters including the physical characteristics of the material and the detection system itself. In a real situation of use, the sensor can experience numerous environmental conditions (source characteristics, air stability, convection, flow, temperature variations). In order to create the coherent set of responses required in the context of this

work, we chose a very simple static laboratory configuration for detection experiments which minimized all these effects (see experimental section). Typical responses obtained for a nitro-aromatic compound and a volatile solvent are shown in Fig. 1a and c.

During a couple of minutes the quartz crystal frequency is first monitored to verify the stability of the system and give the baseline for signal detection. A drop in the response is then recorded almost immediately after introduction of the analyte. It thus decreases and more or less rapidly reaches an equilibrium corresponding to a maximum adsorption. A low Δf and fast adsorption kinetics are typical of most solvents with a high vapor pressure, e.g., butanone (Fig. 1c). Conversely, a high Δf is reached for nonvolatile compounds like dinitrotoluene, but in this case several hours of experiment are required (Fig. 1a). This is potentially the result of both the evaporation kinetics in the detection compartment and the diffusion in the polymer being very slow. In all cases, the original frequency is retrieved after re-exposure to neat air, demonstrating the reversibility of the process which is consistent with the formation of weak noncovalent interactions between the analyte and the sensitive molecule.

3.1.2. Analytes with high saturation vapor pressure

In the Sauerbrey regime, an increase of the deposited mass ($\Delta m > 0$) should produce a reduction of the crystal frequency ($\Delta f < 0$). When the QCM was exposed to a high vapor pressure of a volatile compound with a low viscosity, an intense and rapid variation with an opposite sign up to $\Delta f = 1200$ Hz was observed (Fig. 1b). Such a result has already been reported but the data were given without further details [13]. The opposite sign would suggest that part of the coated material was lost, but this interpretation

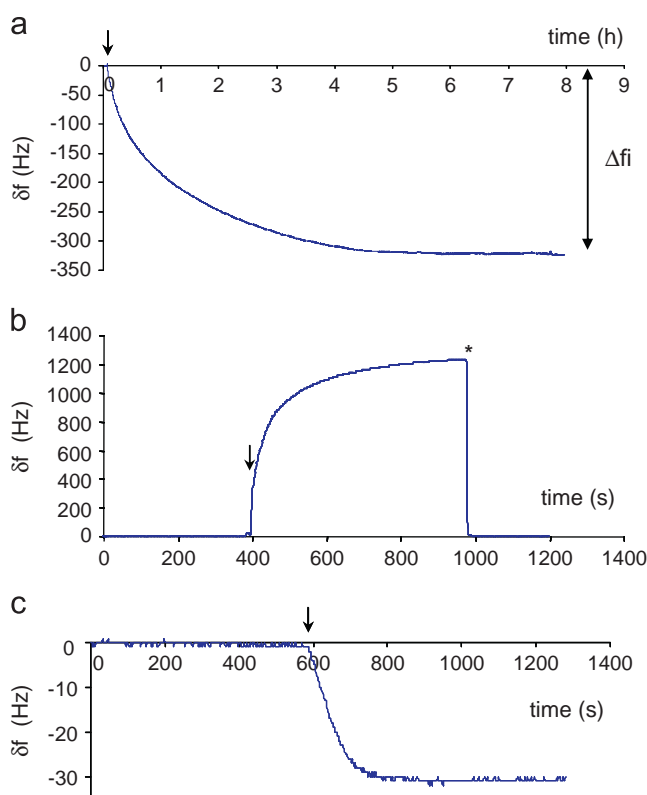


Fig. 1. PCN-coated QCM responses. Frequency variation $\delta f = f(t) - f(t=0)$ as a function of time obtained for a QCM sensor coated with PCN and exposed to a large excess of 2,4-dinitrotoluene (a), a large excess (20 ml) of butanone (b), and 12000 ppm of butanone (c). The time at which the analyte was introduced is marked by an arrow. The star indicates the beginning of desorption that happens after a re-exposure to neat air (shown for case (b) only).

does not hold as the initial frequency was retrieved after a total desorption.

Rather, the phenomenon can be explained as resulting from a modification of the regime governing the frequency variation. For the neat polymer, d_s was estimated at 120 μm which is larger than the dimension of the layer. The frequency variation was thus governed by the linear Sauerbrey regime.

After the adsorption of a large amount of analyte, the viscosity decreases, as does d_s , to such an extent that the frequency variation becomes proportional to $\eta^{1/2}$. The proportionality coefficient α was here determined by immersing the quartz crystal in a series of solvents with different viscosities (not shown). Using α and the known viscosity of butanone, a variation of $\Delta f \approx -2100$ Hz would be expected in comparison with the bare crystal (viscosity vanished). Actually, a variation $\Delta f = 1200$ Hz with regard to the neat polymer was observed. But this was equivalent to a variation $\Delta f = -800$ Hz with regard to the bare crystal since the contribution from the polymer layer itself was close to -2000 Hz. The experimental frequency variation was thus consistent with a microbalance coated with 38% (800 Hz/2100 Hz) of a mixture highly concentrated with butanone. This interpretation seems realistic if a comparison is made with the initial quartz covering of 15% (evaluated from analyses of the images obtained by optical microscopy) and taking into account the volume variation due to the adsorption of solvent.

Fortunately, such a concentration level is unlikely to occur in practical applications. If it did, it would require a confined environment containing an important source of solvent. Moreover, a negative frequency variation, Δf , at equilibrium corresponding to a mass adsorption was retrieved at a reduced vapor pressure of 12,000 ppm (Fig. 1c). Finally, in order to assess the domain of applicability of the Sauerbrey regime, the experiment was repeated by introducing several volumes of liquid butanone and dichloromethane. As expected, Δf was found proportional to the vapor pressure up to a certain limit (Fig. 2). A deviation from linearity was observed near a butanone concentration of 20,000 ppm whereas the limit was still not reached with 80,000 ppm of dichloromethane. As both solvents viscosities are quite similar, a lower limit for butanone is the consequence of a weaker partition coefficient. This is confirmed by the lower frequency variation observed for butanone for a given vapor pressure.

3.1.3. QCM Results

QCM measurements were carried out on five functionalized polysiloxane polymers, PCN, Pph, P8, PpyN and PpyCOO. A full matrix comprising 20 analytes was tested on PCN and only a reduced number of them were retained for the evaluation of the other polymers. Results are gathered in Table 1 together with the vapor pressures used for the measurement. At a first glance, the responses obtained at a given vapor pressure showed a high variability by column, i.e., when different analytes exposed to a given polymer were compared. Conversely, more tenuous differences were seen in each row, i.e., when the various polymers exposed to a given analyte were compared. A quantitative analysis of these results will be discussed in the next section.

3.2. PM-RAIRS measurements

In order to obtain direct insight into the adsorption phenomenon, PM-RAIRS spectra of polymer coatings (PCN, Pph, P8 and the polytrifluoropropylmethylsiloxane denoted as PCF3) were recorded after in-situ exposure to a nitrogen flow containing a certain concentration of analyte. The aim of these experiments was first to show the linear relationship up to a certain vapor pressure between Δf from QCM and the amount of adsorbed

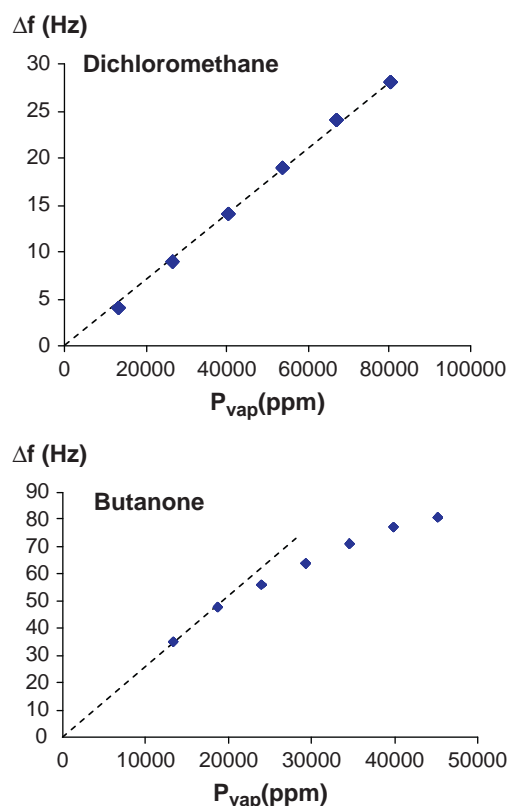


Fig. 2. Linearity of Δf vs. P_{vap} . Evolution of the frequency variation, Δf , as a function of the analyte vapor pressure obtained for a PCN-coated QCM exposed either to dichloromethane or butanone. The dotted lines are merely a guide to the eyes.

analyte, and second to confirm the variability observed in the QCM responses of different compounds.

For nonvolatile analytes such as p-nitrotoluene, phenol, aniline, spectra were recorded at regular intervals during the course of adsorption. The evolution of the adsorbed aniline ratio in PCN as a function of the time of exposure is illustrated in Fig. 3. Although a close similarity with the QCM curves was obtained, variations in the kinetics were generally observed as the conditions of adsorptions differed in both experiments. Following a first adsorption, a desorption was initiated by introducing neat air in the detection compartment, after which the adsorption could be repeated. The good superimposition of the two curves obtained for aniline proves that the desorption was complete and confirmed the total reversibility of the adsorption process.

Fig. 4 displays the intensity variation measured after 1 h for several couples of polymers and analytes.

This graph does not enable the comparison of the intensity values recorded for the various analytes as they depend on different molar extinction coefficients. On the other hand, PM-RAIRS results confirmed that the responses depended on the coated polymer and that this dependency varied with the type of analyte. For two nitro-aromatic compounds with a low saturation vapor pressure P_{sat} , PM-RAIRS and QCM measurements were performed on the same set of four polymers. The proportionality relationship found between both techniques provided a clear demonstration that the frequency variation ΔF measured by QCM was proportional to the mass adsorbed in the polymer deposited on the crystal surface.

Several attempts at recording PM-RAIRS spectra using the same experimental conditions failed when PCN was exposed to a series of highly volatile solvents. For compounds such as dichloromethane, the detection was not possible due to its low IR receptivity.

Table 1
QCM measurements results. Frequency variation at equilibrium Δf measured with QCM detectors obtained for different sensitive materials and analytes. The quartz was successively coated with 2 kHz of PCN, 2 kHz of Pph, 3.1 kHz of P8, 2 kHz of PpyN and 2.4 kHz of PpyCOO. The analytes' vapor pressures (expressed in ppm) produced in the detection compartment are indicated in brackets.

Δf (Hz)	PCN	Pph	ppycoo	p8	pyN
Phenol	840 (473)				
Ethanol	30 (11166)	5 (24755)	12 (24,755)	11 (24,755)	9.5 (24,755)
Acetonitrile	16 (12,483)	1 (27,572)	7 (27,572)	5.3 (27,572)	4 (27,572)
Acetone	12.6 (13,319)		5 (19,587)	5 (19,587)	2 (19,587)
Methylethylketone	28.6 (18,196)				
Dichloromethane	11 (10,171)	3 (10,171)	26 (17,732)	25 (17,732)	11.5 (17,732)
Chloroforme	39.6 (12,222)		26 (22,550)	25 (22,550)	5 (22,550)
Dymethylsulfoxide	461.7 (594)				
Cyclohexane	6.6 (12,069)		14.6 (13,346)	25.3 (13,346)	5.75 (13,346)
Tridecane	40 (80)				
Toluene	41.6 (15,302)		47 (13,597)	75 (13,597)	12 (13,597)
Aniline	650 (841)	99 (841)	90 (841)	91 (841)	79 (841)
Trinitrotoluene	0.0 (0.01)				
2,4-Dinitrotoluene	318 (0.3)				
Nitrobenzene	165 (199)	130 (199)			
o-Nitrotoluene	323.3 (37.5)	1177 (37.5)	75 (37.5)	71 (37.5)	49 (37.5)
p-Nitrotoluene	333 (79.7)		23 (79.7)	31 (79.7)	19 (79.7)
2,4-Dinitrophenol	178 (6)				
H ₂ O ₂	138.3 (1947)				
Nitromethane	51.4 (12,142)				
1-Hexylamine	315 (8700)				
2-Hexylamine	224 (8700)				

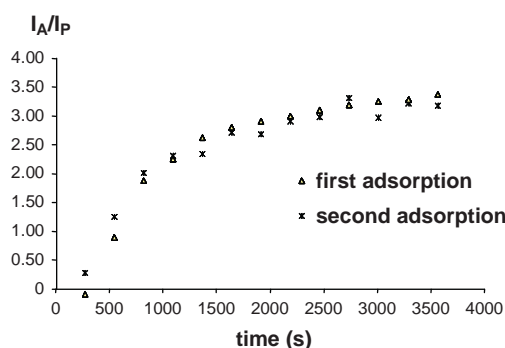


Fig. 3. PM-RAIRS adsorption kinetic measurements. Two adsorption kinetic curves (separated by a desorption period under neat air) of aniline in a PCN coating followed by in situ PM-RAIRS measurements. I_A and I_P are integrations of one adsorption band of each compound.

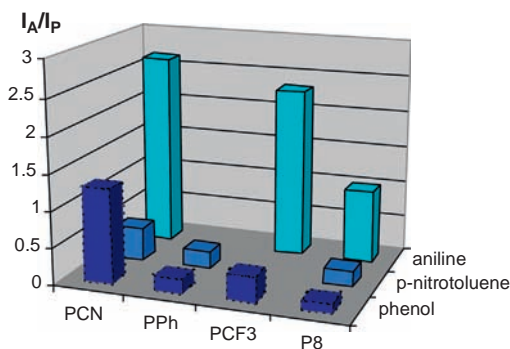


Fig. 4. PM-RAIRS maximum adsorption results. PM-RAIRS I_A/I_P values determined at an adsorption time of 1 h obtained with different analytes and polymers. Missing values are due to problems of leakage during the experiment.

For those bearing IR-sensitive chemical groups like toluene or butanone, spectral saturation led to a bad suppression of the gas contribution from the spectra. Although a slight signal evolution of the nitro group was seen for nitromethane, the presence of artefacts prevented any spectral integration for quantitative analysis.

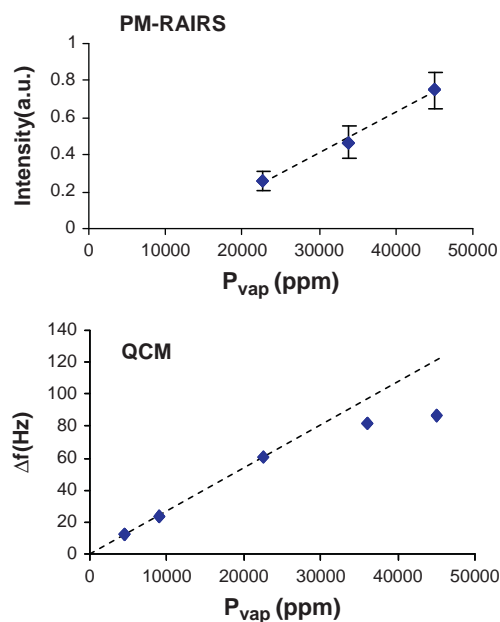


Fig. 5. Comparison of PM-RAIRS and QCM measurements. PM-RAIRS and QCM adsorption of toluene in PCN measured after stabilization following the introduction of three different small volumes of analyte. An air flow was restored before each experiment to clean the detection chamber and enable complete desorption. The IR intensity was obtained by spectral integration of toluene. The shift from the origin (zero intensity at $P_{vap}=0$) was due to the baseline correction procedure.

Drastically reducing the vapor pressure inside the detection chamber provided a unique opportunity to obtain exploitable IR responses of these compounds. Hence, measurements were subsequently performed using a static configuration without flow similar to the one used for the QCM experiments. The detection compartment was physically isolated, a small volume of analyte introduced and spectra recorded at regular intervals until stabilization was reached.

The intensity evolution of toluene adsorbed in PCN as a function of the introduced toluene vapor pressure P_{vap} is displayed in Fig. 5. Although limited to three points, the observed variation

suggests a roughly linear relationship and thus confirmed that the proportionality relationship observed between Δf measured by QCM and P_{vap} (also given in Fig. 5) correlated well with the mass variation of the sensitive polymer layer, even for volatile solvents. The smaller domain of linearity obtained by QCM can be explained by a modification of the viscoelastic properties of the layer at a certain analyte concentration.

Finally, PM-RAIRS measurements rendered it possible to evaluate whether the Sauerbrey equation could be used and to delimitate its domain of validity under the conditions of our experiment. It was shown that the vapor pressure of the analytes had to be maintained below a limit value estimated at 20,000 ppm. Hence, the introduction in the detection chamber of analytes with a $P_{\text{sat}} > 20,000$ ppm was reduced to a few μl whereas nonvolatile compounds could be introduced in excess. Under these conditions, the frequency variation measured by QCM could be considered as proportional to the mass adsorbed in the polymer deposited on the crystal surface.

4. Theoretical interpretation and discussion

4.1. QCM frequency variation at equilibrium

In a solid, the adsorption of a vapor is often restricted to a limited number of sites on the close surface leading to a Langmuir evolution as a function of the concentration in the gas phase with an asymptotic limit. Conversely, species adsorbed on the surface of a polymer oil can rapidly diffuse inside releasing the surface for further adsorption until the chemical potentials in both phases reach the same value. In this situation, Henry's law predicts that the ratio of the concentration in the condensed phase to the concentration in the gas phase at equilibrium is constant and equal to the partition coefficient.

In the linear domain of QCM responses, the partition coefficient can be calculated from the frequency variation at equilibrium, Δf , using the mathematical expression given in reference [4]. The constant K is linked to the Gibbs free enthalpy by the relation $\Delta G_{\text{sorb}} = -RT \ln K$. A first approximation of ΔG_{sorb} can be obtained by considering the adsorption process in two steps [4]: a preliminary condensation of the analyte, assumed as ideal with a contribution ΔG_{cond} , and the mixture of both compounds in the condensed state with a contribution ΔG_{m} . We thus have:

$$-RT \ln K = \Delta G_{\text{cond}} + \Delta G_{\text{m}}. \quad (1)$$

The first term, which is equivalent to $-\Delta G_{\text{vap}}$, can be evaluated for thousands of compounds for which ΔH_{vap} values have been reported in a recent review [14]. The entropic term is not as well documented as it is more difficult and less accurate to measure, but an approximated value can be obtained [15] with the expression $\Delta G_{\text{vap}}(T) \approx \Delta H_{\text{vap}}(T)(1 - T/T_{\text{Eb}})$ assuming that the calorific capacity of both phases is constant in the temperature range $[T, T_{\text{Eb}}]$. ΔG_{vap} was calculated according to the above expression for a set of analytes and then compared to ΔG_{sorb} deduced from QCM measurements performed on two polymers. A linear fit to experimental data was proof that these two terms were reasonably well correlated (Fig. 6).

Fig. 6 confirmed that, as already noticed [4], a less volatile analyte was adsorbed to a larger extent, regardless of the material considered. This was, however, a first approximation as two other effects could also be noticed. First, the fitted curve displayed a slope close to unity but did not intersect the Y-axis at the origin. Second, a dispersion of experimental points was seen around the theoretical line. According to Eq. (1), the distance from the line $y=x$, i.e., the free energy difference $\Delta G_{\text{sorb}} - \Delta G_{\text{cond}}$, should correspond to the free enthalpy of mixing ΔG_{m} . The mixing part also

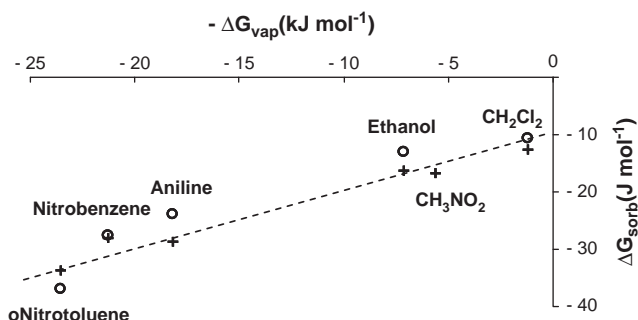


Fig. 6. QCM results vs. vaporization free enthalpy. Comparison between ΔG_{sorb} determined by QCM measurements and $-\Delta G_{\text{vap}}$ calculated from tabulated vaporization enthalpies. The plus signs correspond to PCN and the circles to Pph. The dashed line represents the best linear fit to experimental data.

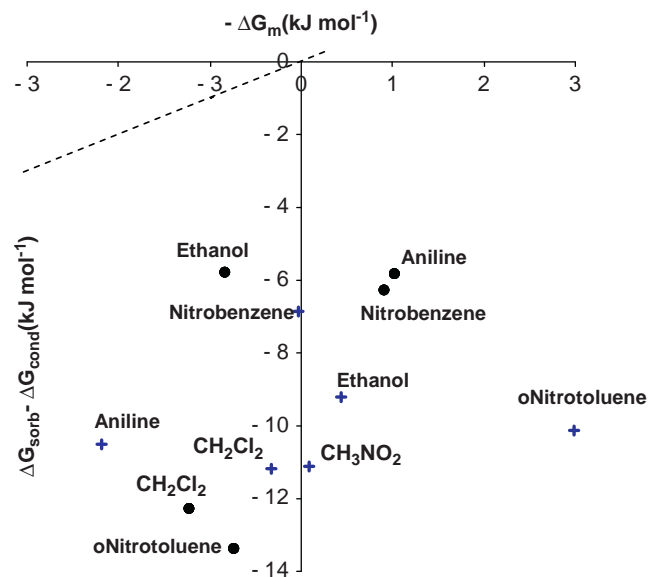


Fig. 7. QCM results vs. mixing free enthalpy. Energy difference $\Delta G_{\text{sorb}} - \Delta G_{\text{cond}}$ as a function of the free energy of mixing, ΔG_{m} , determined by NMR chemical shift measurements on neat binary mixtures. The dashed line corresponds to $y=x$, the plus signs to PCN and the circles to Pph.

has two contributions: ΔH_{m} which depends on differences in interaction energy between like and unlike compounds, and ΔS_{m} which is mainly related to volume differences.

The literature is very sparse when it comes to experimental mixing terms of organic compounds and is limited to dissolution enthalpies obtained by microcalorimetry. We thus compared the free energy difference with the free enthalpy of mixing, ΔG_{m} , determined previously by NMR chemical shift measurements on neat liquid mixtures [8].

As seen in Fig. 7, a strong discrepancy was observed between several binary systems. A residue term R greater than the mixing energy itself thus had to be added to the right part of Eq. (1). Obviously, R depends strongly on the analyte, without regard to the polymer considered. Conversely, similar residues were seen for both polymers with a given analyte (Table 2). The largest difference was found for ethanol and was attributed to the presence of water in the Pph/ethanol binary system which perturbed the NMR chemical shift measurement.

Although the origin of R is unclear, several possible explanations can be potentially considered, such as the approximation made on ΔS_{vap} , the assumption of an ideal condensation by neglecting the surface nature and morphology, and the

Table 2

Free enthalpy residue. Energy difference (J mol^{-1}) $R = \Delta G_{\text{sorb}} - \Delta G_{\text{cond}} - \Delta G_{\text{m}}$ obtained for various analytes with two polymers.

	CH_2Cl_2	o-Nitrotoluene	Aniline	Nitrobenzene	Ethanol
PCN	-10,835	-13,122	-8289	-6847	-9634
Pph	-7980	-12,656	-6873	-7204	-4952

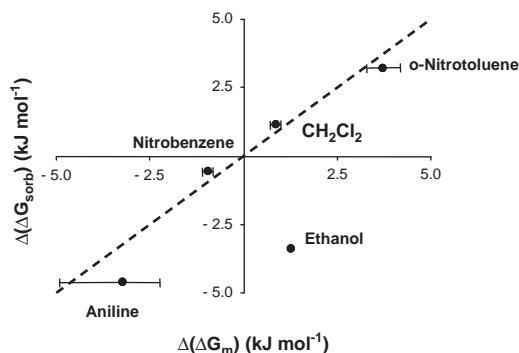


Fig. 8. Differences of free enthalpy, QCM vs. NMR. Difference in free enthalpies obtained for a given analyte and two polymers (PCN and Pph). The sorption term obtained by QCM (y coordinate) has been drawn as a function of the mixing term (x coordinate) determined by NMR. The error bar represents the dispersion resulting from considering the chemical shifts of different couples of atoms. The line $y=x$ is merely a guide to the eye.

modification of the surface tension energy. Of course, explicitly taking into account all these effects would be a very difficult task. Rather, attempts were made to combine ΔG_{sorb} values to minimize their contribution. Assuming that R is essentially analyte-dependent, we calculated the differences between terms that were obtained with a given analyte and two polymers. Consequently, the condensation contribution also vanished and did not require an evaluation from external data, thus leading to a simple formulation depending exclusively on the free enthalpies of mixing: $\Delta(\Delta G_{\text{sorb}}) = \Delta G_{\text{sorb}}$

$$(\text{A, PCN}) - \Delta G_{\text{sorb}}(\text{A, Pph}) = \Delta G_{\text{m}}(\text{A, PCN}) - \Delta G_{\text{m}}(\text{A, Pph}) = \Delta(\Delta G_{\text{m}}).$$

Surprisingly, despite the relative importance of the residue term R , a satisfactory agreement was seen —except for ethanol— between $\Delta(\Delta G_{\text{sorb}})$ and $\Delta(\Delta G_{\text{m}})$ determined from NMR (Fig. 8). The advantage of considering the differences between QCM responses instead of the responses themselves is that only mixing terms have to be evaluated for their prediction. This result must be related to our previous paper where a fairly good agreement was seen between ΔG_{m} values experimentally determined by NMR and those calculated from the Hansen formalism based on the solubility coefficients.

4.2. Kinetics of the response

QCM detection experiments were carried out using a confined atmosphere of gas without flow. Under such conditions, the adsorption of the analyte in a polymer above its glass transition temperature is governed by Fick's law of diffusion [16]. Hence, the concentration in the condensed phase is driven by the relation: $c_t/c_\infty = (4/h)\sqrt{D \cdot t/\pi}$ where c_∞ and c_t are the analyte concentrations in the polymer at equilibrium and at a given time t , respectively, D is the diffusion coefficient of the analyte in the polymer and h is the polymer thickness. D can be easily evaluated by the mathematical expression $D = \pi(h\theta/4c_\infty)^2$ where θ is the initial slope of the diffusion curve drawn as a function of $t^{1/2}$. D was determined in this manner when possible, i.e., for analytes presenting a sufficiently slow diffusion in PCN. Corresponding

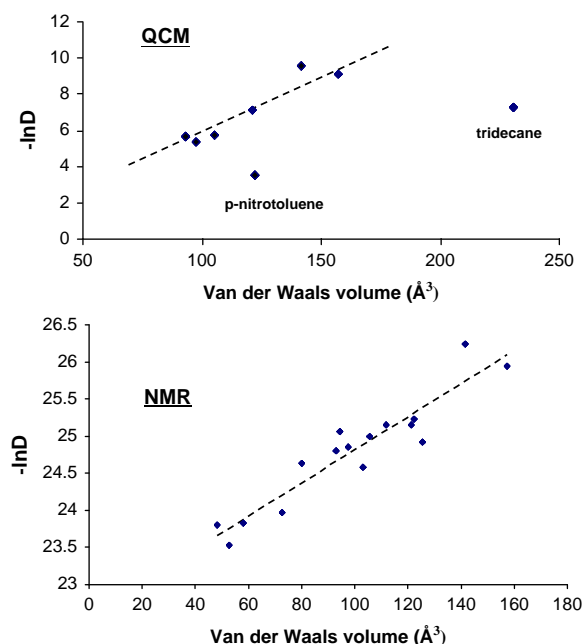


Fig. 9. Diffusion coefficient vs. Van der Waals volume. Evolution of $\ln(D)$, i.e., the natural logarithm of the diffusion coefficients of the analytes, as a function of their Van der Waals volume (calculated using Hyperchem with a PM3 algorithm). (top) The D values were determined from QCM measurements; (bottom) D represents the self-diffusion coefficient measured by NMR on highly diluted solution of analyte in neat PCN [8]. The continuous line represents the best linear fit to the experimental data excluding the two singular points.

$\ln(D)$ values are displayed in Fig. 9 as a function of the Van der Waals volume, V_a .

With the exception of two singular points (one of which is the tridecane molecule which has a different diffusion behavior due to its particular shape and size), and within experimental errors, $\ln(D)$ is fairly proportional to V_a . A similar observation has already been reported and used in a mathematical procedure aimed at discriminating analytes [17]. A linear dependence on V_a has also been observed on the self-diffusion coefficients measured by NMR on a series of organic compounds highly diluted in PCN (Fig. 9) but the slope and origin were different.

This difference can have at least two origins: (i) in the QCM measurements the adsorption kinetics are driven by the Fick diffusion coefficient that differs from the NMR self-diffusion coefficient at finite dilution; (ii) if the vaporization of the analyte is slower than the adsorption in the polymer at ambient temperature, it can control the whole process. In that case, an apparent diffusion coefficient lower than the Fick coefficient is observed.

In this section, it has been shown that the Fick diffusion coefficient of an analyte adsorbed in a polymer can be evaluated from its Van der Waals volume, a parameter that can be easily obtained from the literature or simple calculations. According to the figures above, this approximation holds true for sufficiently compact and small analytes presenting isotropic motion. Linear systems like alkyl chains presenting highly anisotropic displacements need a more sophisticated calculation. Hence, c_t , i.e., the concentration of adsorbed analyte at any time t can be easily predicted from c_∞ , i.e., the concentration at equilibrium, an evaluation of which has been given in the first section from mixing enthalpies. It is thus readily possible to extend a prediction model built on a thermodynamic basis to a real situation of use of a sensor. This is due to a complete adsorption often not being reached since, for practical reasons, the detection process is limited to a few minutes.

5. Conclusion

This paper has described the investigation of the QCM responses of various functionalized polysiloxane layers exposed to a series of compounds in the gas phase. The free enthalpy of sorption has been determined from the partition coefficient and brought together with the free enthalpy of mixing deduced from NMR measurements carried out with neat mixtures. A comparison with thermodynamic data from the literature has led us to consider two limiting cases (i) first, by restricting the measurements to a single material, the free enthalpy of sorption, ΔG_{sor} , could be approximated to the free enthalpy of vaporization, ΔG_{vap} , of the analyte; (ii) second, to deal with several materials, a simple expression linking ΔG_{sor} and the free enthalpy of mixing, ΔG_{m} , was obtained by calculating differences between two materials and the same analyte. Moreover, an equivalence has been shown previously between mixing terms determined by NMR and those calculated using Hansen formalism. These two main conclusions were the starting point for the development of predictive models presented in another paper. To deal with the practical situation of detection restricted to short times, we showed that a diffusion coefficient

estimated from the Van der Waals volume could be used for small molecules.

References

- [1] A. Hulanicki, S. Glab, F. Ingman, *Pure Appl Chem.* 63 (9) (1991) 1247–1250.
- [2] K.G. Furton, L.J. Meyers, *Talanta* 54 (2001) 487–500.
- [3] R.A. Potyrailo, V.M. Mirsky, *Chem. Rev.* 108 (2008) 770–813.
- [4] A. Hierlemann, A.J. Ricco, K. Bodenhöfer, A. Dominik, W. Göpel, *Anal. Chem.* 72 (2000) 3696–3708.
- [5] D. Johannsmann, *Phys. Chem. Chem. Phys.* 10 (2008) 4516–4534.
- [6] W.H. King, *Anal. Chem.* 36 (9) (1964) 1735–1739.
- [7] L.R. Khot, S. Panigrahi, D. Lin, *Sensors Actuators B* 153 (1) (2010) 1–10.
- [8] J. Klingenfus, P. Palmas, *Phys. Chem. Chem. Phys.* 13 (2011) 10661–10669.
- [9] J.M. Chalmers, P.R. Griffiths, *Handbook of Vibrational Spectroscopy—Sampling Techniques*, vol. 2, John Wiley and sons, Chichester, 2002.
- [10] S. Clavaguera, P. Montmeat, F. Parret, E. Pasquinet, J.P. Lère-Porte, L. Hairault, *Talanta* 82 (4) (2010) 1397–1402.
- [11] G. Sauerbrey, *Z. Phys.* 155 (1959) 206–222.
- [12] C. Verdier, P.-Y. Longin, M. Piau, *Rheol. Acta* 37 (3) (1998) 234–244.
- [13] Z. Ying, Y. Jiang, X. Du, G. Xie, J. Yu, H. Tai, *Eur. Polym. J.* 44 (2008) 1157–1164.
- [14] J.S. Chickosa, W.E. Acree, *J. Phys. Chem. Ref. Data* 32 (2) (2003) 519–878.
- [15] J.N. Spencer, A.J. Voigt, *J. Phys. Chem.* 72 (1968) 471–474.
- [16] S.N. Zhurkov, *J. Tech. Phys.* 24 (5) (1954) 797–810.
- [17] R.M. Sobel, D.S. Ballantine, *Anal. Chim. Acta* 608 (2008) 79–85.